

ELECTRONIC PROPERTIES OF JUNCTIONS BETWEEN ALUMINIUM AND POLYANILINE DOPED WITH DODECYLBENZENE SULPHONATE

Bantikassegn Workalemahu

Department of Physics, Addis Ababa University, P.O. Box 1176, Addis Ababa, Ethiopia

(Received April 5, 1999; revised May 29, 1999)

ABSTRACT. Polyaniline (PANI) doped with dodecylbenzene sulphonate (DBS) anions forms a conducting organic solid. Aluminium contacts to PANI(DBS) polymer are studied using complex impedance spectroscopy, current-voltage and capacitance-voltage characteristics measurements. The I-V characteristic is asymmetric and non-ohmic and shows rectification. The C-V measurements show that the dopant profile is not uniform throughout the polymer. The complex impedance spectra show two partially overlapping semicircles which reveal the existence of two distinct regions at the metal/doped polymer interface. They are modelled by an equivalent circuit consisting of two parallel RC circuits in series representing a thin interfacial insulating (S') layer and a depletion (S) region. The device is therefore an MS'S type, where S' and S are the same chemical compounds having different dopant concentrations.

INTRODUCTION

Metal contacts to semiconductors form interfaces that give basic features of many rectifiers, metal-semiconductor and metal-insulator-semiconductor devices such as field-effect transistors, sensors, and other surface junction devices. Thus electrical contacts to semiconductors are critical elements in a number of important technologies.

A significant amount of research has been carried out on the use of semiconducting polymers, in neutral as well as doped states, as active materials in electronic and optoelectronic devices. The overall quantum efficiency of polymer-based light-emitting diodes (PLEDs) is strongly influenced by the injection of electrons and holes at the respective metal/polymer interface [1]. Usually indium-doped tin oxide (ITO) coated glass is used as a hole injecting contact, while the counter electrode is a metal having work function lower than that of the polymer that enables electron injection into the conduction band of the polymer. In this context, the overall device efficiency may be limited by the injection efficiency of the minority carriers. There has been a breakthrough in the area of PLEDs [2-4]. For instance, multicolour PLEDs were made from side-chain substituted thiophene polymers exhibiting electroluminescence over the full visible spectrum, from the blue into the near-infrared [3]. White light emission from Al(or Mg)/PANI/ITO is also reported [5].

Doping increases the electrical conductivity of conjugated polymers [6]. Despite numerous reports on devices that utilize conjugated polymer-metal contacts, relatively little has been done to investigate the fundamental properties of heterojunctions or metal contacts involving doped conjugated polymers. Polyheterocyclic polymers like polypyrrole (PPy) and polythiophene (PT) can be oxidized to bring them into their highly conducting states. Thus conduction takes place via hole polarons or hole bipolarons, at least for intermediate doping levels. Yet there is little information on the mechanisms that control charge carrier transport at interfaces between metals and the doped polymers, where chemistry induced defects formed when metal atoms are deposited on the conjugated polymer surface are likely to play a crucial role [7-9].

Some interdisciplinary studies of polymer-metal interfaces showed that, during the early stages of interface formation, deposited aluminium atoms form covalent bonds with the carbon of the α -linkage in polythiophenes [10]. Others also reported that low work function metals such as Al or Ca readily react with oxygen-containing parts of the polymer or polyelectrolyte, thus forming a thin resistive layer [9].

Polyacetylene was not only found to be the first conducting polymer [6], but was also the first polymer to be tested as a semiconductor in a diode [11]. Subsequent improvements in synthesis, stability, and diode processibility have led to numerous studies on polymeric diodes made from, for example, thiophene oligomers [12-14] and poly(3-alkylthiophene) [15-19]. These Schottky diodes, however, were made from undoped or unintentionally doped conjugated polymers having low electrical conductivity, and therefore, had currents at forward bias that were limited by bulk resistance.

We have investigated a series of polymer-based structures for which one of the electrodes is a vacuum evaporated aluminium layer. Two-terminal devices based on junctions between p-type conducting polymers doped with large polymeric anions such as polystyrenesulphonate (PSS⁻) and low work function metals, e.g., aluminium, show symmetrical but non-ohmic current-voltage characteristics [8,9,20,21]. For instance, when poly(3,4-ethylenedioxy thiophene), PEDOT, and PPy are doped with PSS⁻ anions, the Al/PEDOT and Al/PPy contacts show metal-insulator-semiconductor (MIS) type of junctions [12,13,20,21]. The same polymers doped with small anions such as perchlorate (ClO₄⁻) [8,9,20,21] and poly[3-(4-octylphenyl)-2,2'-bithiophene], PTOPT, doped with PF₆⁻ give a metal-semiconductor (MS) type contacts. PTOPT, which is one of the derivatives of thiophene, shows Schottky-type high rectification [22].

Generally, the high conductivity of organic polymers lies in their level of conjugation; the more extensive the conjugation, the higher the conductivity. PANI is a peculiar polymer having different oxidation states with varying conjugation levels, namely, leucoemeraldine, protoemeraldine, and emeraldine base polyanilines. The three oxidation states can either partially or fully be protonated, where the nitrogen atoms that bridge the backbone benzene rings are the protonation sites. By virtue of its stability, and particularly high conjugated π -system, emeraldine base PANI doped with DBS is tested in this work as a semiconducting material in a device. We report here the electrical properties of junctions between aluminium and PANI doped with DBS in the form of Al/PANI(DBS)/ITO sandwich structure. The oxidized PANI is a p-type semiconductor, and therefore, hole (bi)polarons are active in charge transport. Complex impedance spectroscopy, capacitance-voltage as well as current-voltage measurements are used for characterizing the electronic properties of the junction.

EXPERIMENTAL

ITO on glass was partly covered with photoresist, and the exposed part of ITO was etched with a mixture of concentrated HCl, HNO₃ and water, 48:4:48 by volume, respectively. The etched portion of the ITO/glass provided a region convenient for electrical contacts to the aluminium layer deposited later. The photoresist was removed using acetone, and then the surface was washed with detergents and distilled water, and rinsed with ethanol.

Emeraldine base polyaniline doped with dodecylbenzene sulphonate was used as received from Netse Oy of Finland. It was dissolved in xylene at a 1:3 ratio by weight and stirred using a magnetic stirrer for about six hours, until a thick, black solution was obtained. This solution was then centrifuged for about two hours, at the end of which a clear yellowish and slightly

viscous solution was separated and stored in a clean and cold environment. Using a spinner system, PANI(DBS) was spin-coated over the ITO/glass substrate from the xylene solution at the rate of 1000 rpm yielding uniform, high quality yellowish thin films, whose thickness were estimated from the concentration and spin rate to be about 200 to 300 nm.

About 500 nm thick aluminium strips were vacuum deposited at a pressure of 1.0×10^{-6} Torr as the required low work function metal contact to PANI(DBS). Part of the Al strip was over the PANI(DBS)/ITO, while the remaining part was over the glass from which the ITO was etched out. This was to avoid possible damage of Al and the polymer beneath when electrical contacts were made. The active area was about 0.1 cm^2 . The diode is forward biased when the aluminium electrode is connected to a negative voltage. The sandwich structure of Al/PANI(DBS)/ITO provided a means of current-voltage, capacitance-voltage and complex impedance measurements. The samples were kept in the dark, at room temperature in dry air during all measurements.

Current-voltage characteristics were measured with HP 4145B semiconductor parameter analyzer together with HP 16058A test fixture. The applied voltage was scanned between -5 V and 5 V. A computer interfaced HP 4129A LF impedance analyzer was used to measure the C-V and complex impedance. During C-V measurements, the frequency was kept at 1 kHz. In impedance measurements the bias voltage applied to the diode ranged between -3 V and 3 V, in steps of 1 V. For every bias voltage used a sinusoidally oscillating voltage of $V_{\text{rms}} = 10 \text{ mV}$ was applied. The frequency was scanned between 500 Hz and 10^7 Hz for each bias. With the help of the EQUIVCRT programme [23], Cole-Cole plots were generated and analyzed.

RESULTS AND DISCUSSION

Doping (in most cases oxidation) of polymers creates new electronic states in the energy gap. The presence of these states in the otherwise forbidden gap provides new optical transitions, in addition to the inter-band transition. The transition from the valence band to these new band-gap states is referred to as the bipolaron transition because polarons are rarely observed, since it is energetically favourable for the polarons to combine and form bipolarons [24].

Current-voltage characteristics. Figure 1 shows the current density-voltage characteristics of the Al/PANI(DBS)/ITO device in the dark. The forward bias voltage corresponds to the Al being negative. The J-V curves are asymmetric and non-linear, with increasing forward current at low voltage regions. The device exhibits a rectifying behaviour in the dark with a turn-on voltage at about +1 V (see Figure 2). This rectification property can be attributed to the formation of a depletion region at the interface between the aluminium and the polymer (see *complex impedance analysis*).

According to the Schottky barrier theory [25], p-type semiconductors form rectifying barriers at the interface when the work function of the metal is smaller than that of the semiconductor. However, if the work functions of both electrodes are greater than that of the semiconductor, the junction gives an ohmic I-V curve (rather than rectifying) [8]. Since PANI doped with DBS behaves as a p-type semiconductor, its work function is in between that of the Al (4.1 eV) and the ITO (4.9 eV) yielding a rectifying contact with aluminium. A semilogarithmic plot (Figure 2) of the forward current density (J) versus the applied voltage (V) shows that the forward current increases exponentially in the applied voltage region between 1 V and 2 V, which indicates the formation of the depletion region between the Al and the polymer.

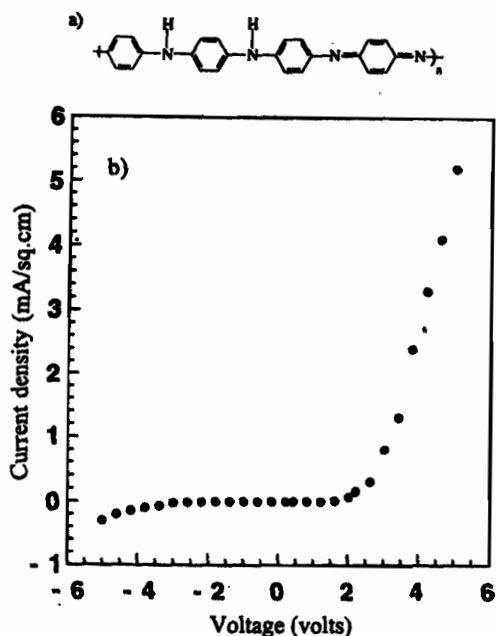


Figure 1. a) The chemical structure of emeraldine base PANI; b) J-V characteristic of an Al/PANI(DBS)/ITO device.

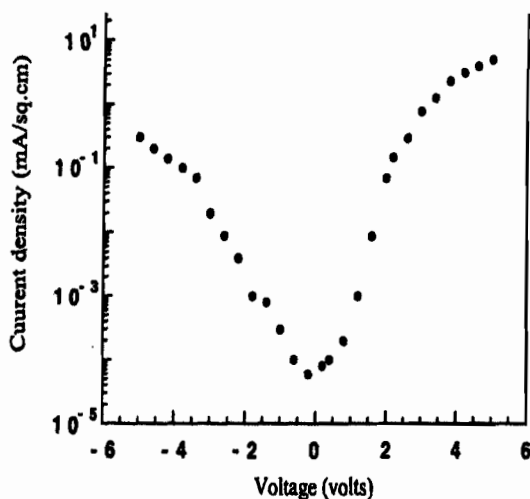


Figure 2. The semilog plot of the J-V curve shown in Figure 1(b).

A Schottky barrier device with rectifying J-V behaviour is usually assumed to follow the standard thermionic emission theory for conduction across the junction [25]. In this theory the current is controlled only by the transfer of charge carriers across the interface of

Al/PANI(DBS). The current density-voltage relationship for the Schottky barrier diode is given by

$$J = J_0[\exp(qV/nkT) - 1] \quad (1)$$

where J is current per unit area, J_0 the reverse saturation current density, q the electronic charge, V the applied forward voltage, T the absolute temperature, k the Boltzmann constant, and n the ideality factor of the diode.

The barrier height, ϕ_b , can be deduced from the reverse saturation current density, J_0 , using the Richardson equation [26]:

$$J_0 = A^*T^2 \exp(-q\phi_b/kT) \quad (2)$$

where A^* is the effective Richardson constant taken to be $120 \text{ Acm}^{-2}\text{K}^{-2}$ for a free electron. This value is usually assumed for a Schottky diode with p-type organic semiconductor in barrier height calculations [26,27]. When J_0 is very small compared with the current density of experimental interest, the contact will effectively block current flow for the reverse bias voltage. Such a device will also display an exponentially increasing current when a forward bias voltage is applied. When all other factors are held constant, and $J \gg J_0$, then the diode will have high rectification ratio. For such a low value of J_0 , the barrier height, ϕ_b , is considered high. This phenomenon occurs when low work function (electropositive) metals are in contact with p-type semiconductors [28].

From equation (1), with the condition that $qV \gg kT$, the plot $\ln J$ versus V is expected to be linear, in the vicinity of the turn-on, with the intercept of extrapolated linear part of the curve with the $\ln J$ axis corresponding to J_0 . All I-V measurements may involve more than one type of charge transport mechanism such as tunnelling [18], generation-recombination, and leakage currents [29]. As observed from the semilogarithmic plot of the J-V curve, there could be more than one mechanism of charge transport. It is therefore difficult to choose the linear range that corresponds to the exponential increase of the current at a forward bias. The upper limit of the interval is influenced by the series resistance which is indicative of electrical transport dominated by space charge limited current (SCLC) [13,30], while possibly other charge transport mechanism pushes the lower interval limit up, thus reducing the linear region. A linear relationship in the forward bias suggests the formation of a Schottky-type barrier. At higher voltages the current is limited by the ohmic losses in the resistive PANI(DBS) film. The reverse saturation current density, J_0 , (equation (2)) obtained from the intercept of the linear plot of Fig. 2 is $8 \times 10^{-7} \text{ A/cm}^2$. The barrier height calculated from equation (2) is $\phi_b = 0.78 \text{ eV}$. From the exponential slope, the ideality factor n is found to be 2.6. When $n = 1$ the Schottky barrier is ideal, whereas for higher values, e.g., $n \geq 2$, a mid-gap recombination of electrons and holes occurs. The rectification ratio, $\gamma = 20$, (see Table 1).

Capacitance-Voltage characteristics. A linear plot of $1/C^2$ versus V is shown in Figure 3. The data of C-V measurements were taken at a fixed frequency of 1 kHz. The applied reverse bias voltage was between -3 V and 0 V. Mott-Schottky relationship (equation 3) is used to determine the dopant concentration for a simple Schottky type diode [26].

$$C/A = [(q\epsilon_0\epsilon_r N_d)/2 (1/(V_{bi} + V))]^{1/2} \quad (3)$$

which gives a linear variation of C^{-2} with the dc bias voltage (V) in the reverse direction, where C is the effective capacitance, V_{bi} the built-in potential obtained as an intercept of the linear curve with the V -axis, A the electrode area in (cm^2), ϵ_r ($= 3$) the relative permittivity of the polymer, ϵ_0 the permittivity of free space, N_a the dopant concentration determined from the slope of the C^{-2} versus V curve, and q the electron charge. The parameters are listed in Table 1.

Table 1. Electrical parameters obtained from the I-V and C-V measurements of a Schottky-type diode when PANI doped with DBS is used as a semiconductor.

J_n (A/cm^2)	V_{bi} (V)	N_a (cm^{-3})	ϕ_n (eV)	n	γ
8×10^{-7}	1.3	3.3×10^{18}	0.78	2.6	20

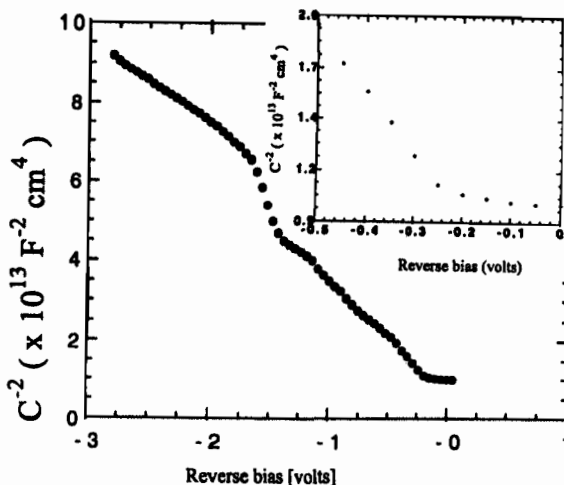


Figure 3. The capacitance-voltage curve of Al/PANI(DBS)/ITO diode. The inset shows the saturation of the C-V data at small values of reverse bias.

The plot of $(C/A)^{-2}$ versus V , as seen from Figure 3, is not a single straight line except in narrow voltage regions. Taking the data in the range between -1.7 V and -3 V, and approximating this with a linear function, the built-in voltage is about 1.3 V. The dopant concentration obtained from the slope for the same voltage range is about $3.3 \times 10^{18} \text{ cm}^{-3}$. Moreover, the value of $1/C^2$ almost saturates at reverse bias voltages close to zero. This indicates that there is an additional capacitance in series with the variable space-charge capacitance of the polymer, which limits the capacitance of the structure at reverse bias voltages close to zero. The linear regions have slightly different slopes that indicate a slight variation of doping concentration. The nonlinear region with the decreasing derivative at small reverse bias voltages shows an entirely different dopant profile, (see the inset of Figure 3), different from the dopant concentration of the bulk. This is consistent with features obtained from complex impedance measurements. The step at -1.5 V is perhaps a smooth connection between the values of the two capacitances as the result of continuous measurements. Its physical significance is not clear yet.

Complex impedance analysis. To gain insight into the nature of the junction and to obtain an equivalent circuit model for the diode, we characterized the Al/PANI(DBS)/ITO thin film device by measuring the complex impedance as a function of frequency and bias voltage. Theoretically a Cole-Cole plot of complex impedance is a semicircle whose center, the “zero-frequency” and the “infinite-frequency” intercepts lie on the Z_{real} axis [31]. Usually the zero-frequency real impedance in most measurements is obtained by extrapolation. The Cole-Cole plots thus generated are depressed semicircles, each point being characteristic of a certain frequency value of measurement.

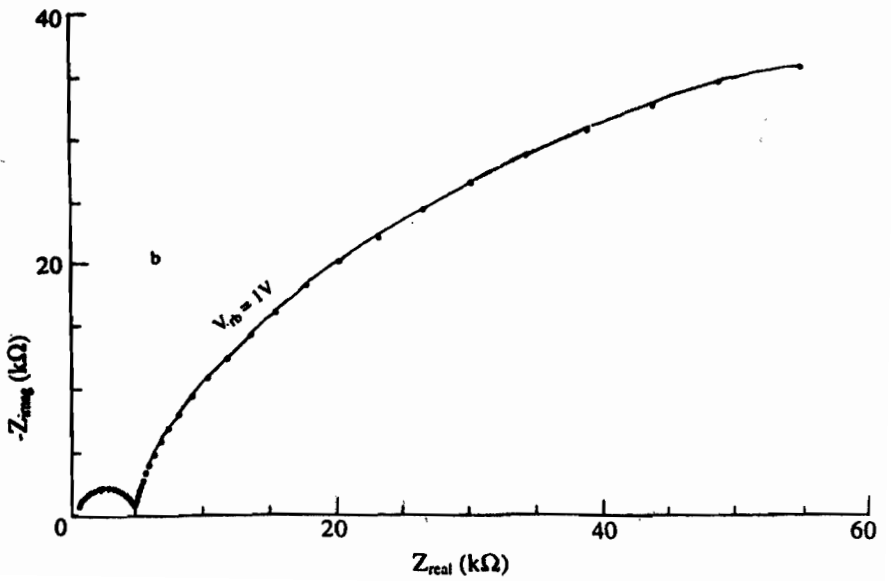
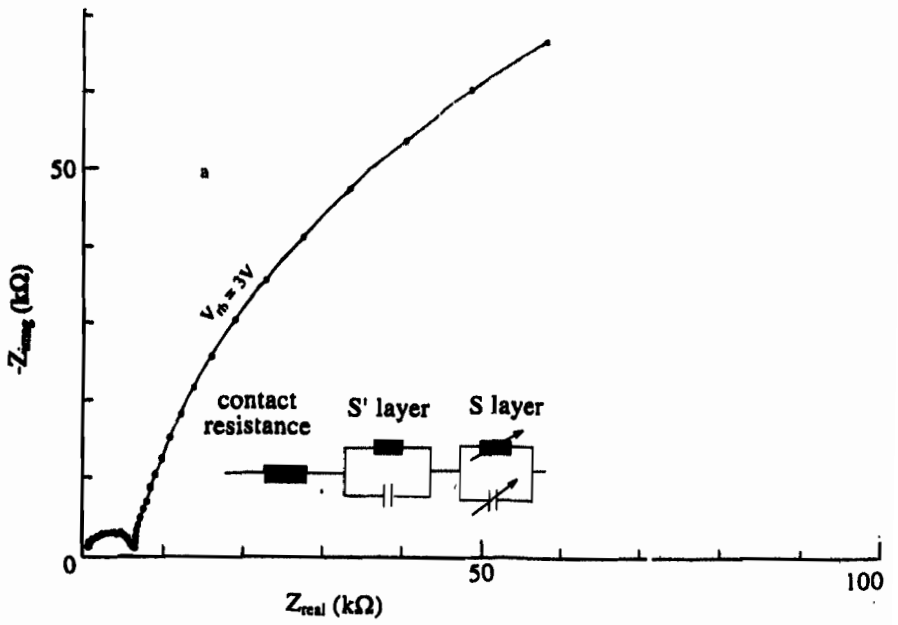
While recording the complex impedance spectroscopy, the frequency is scanned between 500 Hz and 10^7 Hz in a logarithmic sweep at 10 points per decade for each bias voltage. The applied dc voltages to the aluminium electrode are -3 V, -2 V, and -1 V (reverse bias), and +1 V, +2 V, and +3 V (forward bias). For every bias voltage used, a sinusoidally oscillating voltage of $V_{rms} = 10$ mV is applied. Figure 4 shows the Cole-Cole plots of these measurements which reveal portions of two partially overlapping depressed semicircles in a complex impedance plane. The filled points are the measured co-ordinates of the real and imaginary parts of the impedance.

Diodes are commonly analyzed by using an equivalent circuit model as shown in the inset of Figure 4(a). The two semicircles are modelled by two parallel RC circuits in series. The value of the resistance at the highest frequency, which is obtained from the intercept of the curve with the Z_{real} axis, is merely the contact resistance. The left semicircle at high frequency represents a thin interfacial insulating layer, which we label S'. The larger (low frequency) right semicircle, labelled S, represents the depletion region which depends on the applied bias voltage. The slight variation of S' layer with the applied voltage is possibly due to the result of its overlap with S layer, which is strongly bias voltage dependent. Thus the Al/PANI(DBS) interface may be interpreted as a metal-insulator-semiconductor (MIS) junction, or analogously as an MS'S type junction, where S' and S are the same chemical compounds with different dopant concentrations [12,13,20,21].

With the help of the EQUIVCRT programme, a circular fit for the complex impedance representation is performed, where the constant phase element (CPE), $Q = 1/[(j\omega)^n C]$, is used to estimate the value of the capacitance. When $n = 1$, the fit is ideal, and Q represents the imaginary component of the impedance yielding the corresponding capacitance C. In estimating the parameters from the Cole-Cole plots, the value of the relative permittivities for oxides of aluminium and the polymer are taken as 9 and 3, respectively. The parameters from the Cole-Cole plot are listed in Table 2. The resistance of the depletion regions (R_s) and the corresponding depletion width (d) for S layer decrease with increasing bias voltage, being largest at the highest reverse bias ($R_s = 150$ k Ω , and $d = 166$ nm at -3 V) and smallest at the highest forward bias ($R_s = 34$ k Ω , and $d = 31$ nm at +3 V). This is consistent with the J-V rectification characteristics. The corresponding capacitance (C) increases.

Table 2. Parameters obtained from the Cole-Cole plots of the Al/PANI(DBS)/ITO device. The negative sign represents the reverse bias voltage, while others are specified in the text.

V_b (volts)	R_s (k Ω)	C_s (nF/cm ²)	R_s' (k Ω)	C_s' (nF/cm ²)	d (nm)	
					S	S'
-3	150	16	6	130	166	61
-1	85	53	5	320	50	25
1	60	80	6	210	33	38
3	34	83	8	320	31	25



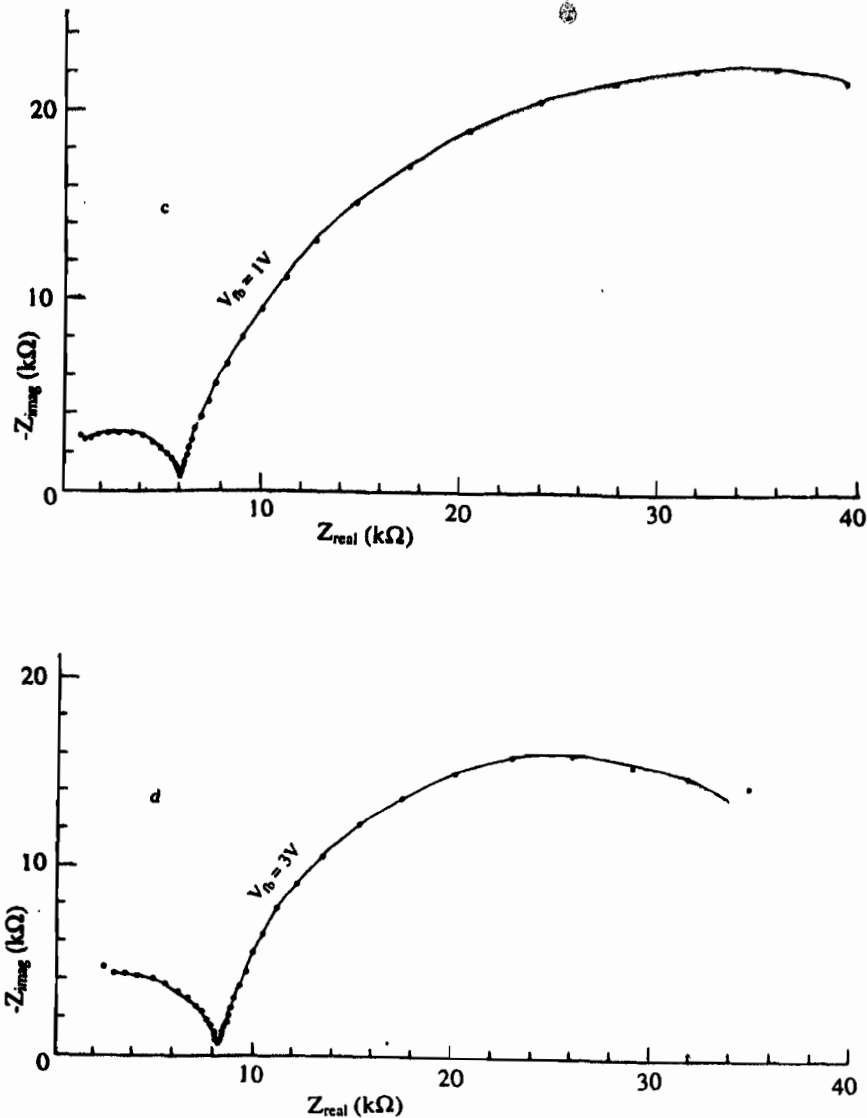


Figure 4 (a-d). The Cole-Cole plots of Al/PANI(DBS)/ITO sandwich structure. The electrical circuit model is shown in the inset of Figure 4(a).

There are several possible factors that cause the formation of the interfacial insulating thin (S') layer between Al and the bulk of the polymer. One important fact that needs to be considered, especially as many studies dealing with metal-polymer inter-phases evaporate low work function metals in a vacuum of 10^5 to 10^6 Torr, is the formation of oxides of the deposited metals. Auger profiling analysis of Ag/PPy and Al/PPy interfaces was reported [32] to manifest the formation of an insulating intermediate phase in the case of Al/PPy due to the

oxides of aluminium between the metal and the polymer. The amount of oxygen present in the polymer is more than sufficient for the formation of insulating oxide at the Al/PPy interface. However, the Au/PPy junctions showed only distinct metal and polymer phases [32]. Moreover, reactions between aluminium and doped polymers are not unexpected. For instance, XPS and He(I)-UPS studies have shown that Al strongly reacts with conjugated polymers at the interface, which leads to the formation of sp^3 -carbon sites that induce the re-orientation of the molecular backbone [7].

Other reports reveal that the distribution of dopants is inhomogeneous in the semiconducting polymers and can be changed by the application of bias voltage [33]. Evaporation of reactive metals such as indium or aluminium is also observed to dedope the polymer at the interface [12,13]. In such cases, there appear to be two regions of the polymer film, a highly resistive thinner (S') layer adjacent to the metal with much lower dopant concentration, and the depletion region of the rest of the film. The structural, chemical, and electrical properties of such interfaces play an important role in charge transport processes because the tendency of dopants to migrate in conjugated polymers might also lead to spontaneous undoping, thereby forming a graded dopant profile.

Junctions between metals and doped polymers in Schottky diodes are expected to form no (or negligibly thin) barriers [22]. Analysis of capacitance-voltage measurements on these diodes based on neutral, or unintentionally doped, polymers leads to acceptor densities N_A of the order of 10^{17} cm^{-3} and a depletion width at equilibrium of about 30 nm. However, for highly doped polymers the acceptor densities are estimated to be of the order of 10^{21} cm^{-3} . Assuming the depletion width to scale as the square-root of the acceptor density [25], a depletion width of about 1 nm or less is expected for devices based on highly doped polymers. Hence, charge transport may be dominated by tunnelling [9,27].

Finally, electrical properties of junctions between doped polymers and reactive metals are influenced by dopant size. An important parameter that determines such a difference is the mobility of dopant anion. Reports reveal that small counterions such as PF_6^- , ClO_4^- [20,22], and BF_4^- [34] move in and out of the polymer matrix during oxidation and reduction processes, while no such detectable difference occurs in the behaviour of large polymeric dopants [34]. In the case of dopant DBS, which is relatively neither small nor large, there could be a significant effect of the electric field on the mobility. A simple estimate of the electric field ($E = V/d$) in the junction between the metal and the polymer yields 10^6 to 10^7 Vcm^{-1} for a depletion width of 10 nm to 1 nm at 1V. In this field even the low ionic mobility of $10^{-13} \text{ cm}^2\text{V}^{-1}\text{s}^{-1}$ [35] will give an ionic drift velocity of about 10 nm/s, high enough to change the profile of doping in a very short time. This may be a general mechanism affecting charge transport in metal/doped polymer junctions, for instance, in the work also reported by the Phillips group [12,13]. However, further investigation is necessary to verify the mechanism.

CONCLUSION

We have constructed a Schottky type device consisting of a vacuum deposited low work function metal (aluminium) on polyaniline doped with dodecylbenzene sulphonate. The thermionic emission model has been applied in order to interpret the J-V and C-V characteristics, from which it was possible to obtain parameters listed in Table 1, and that the Al/PANI(DBS)/ITO structure is a rectifying device. The C-V measurements indicate the inhomogeneous doping concentration due to possibly the dopant migration upon applying bias voltage. The complex impedance spectroscopy shows a thinner resistive (S') layer

between the metal and the depletion region of the doped semiconducting polymer (S) layer as a result of reaction between Al atoms and the constituents of the polymer. The existence of two distinct regions, namely, the left semicircle representing the insulating (S') layer, and the right semicircle representing the depletion region (S layer) of the doped semiconducting polyaniline film is evidenced by the two slightly overlapping depressed semicircles. The S layer is bias-voltage dependent. This structure may be considered as an MS'S rectifying device, modelled by an equivalent circuit consisting of two parallel RC circuits in series, representing the S' and the S layers.

ACKNOWLEDGEMENTS

This work is supported by the International program in the Physical Sciences (IPPS) of Uppsala University under the Project IPPS-ET:01. The author is a Regular Associate Member of the Abdus Salam International Centre for Theoretical Physics (AS-ICTP), Trieste, Italy, where the final part of this work was done, and he thanks AS-ICTP and Sida of Sweden for supporting his visit.

REFERENCES

1. Parker, I.D. *J. Appl. Phys.* **1994**, 75, 1656.
2. Burroughes, J.H.; Friend, R.H.; Burn, P.L.; Holmes, A.B. *Nature* **1990**, 347, 539.
3. Berggren, M.; Ingnas, O.; Gustafsson, G.; Rasmusson, J.; Andersson, M.R.; Hjertberg, T.; Wennerstrom, O. *Nature* **1994**, 372, 444.
4. Gustafsson, G.; Cao, Y.; Treasy, G.M.; Klavetter, F.; Calaneri, N.; Heeger, A.J. *Nature*, **1992**, 357, 477.
5. Chen, S.-A.; Chuang, K.-R.; Chao, C.-I.; Lee, H.-T. *Synth. Met.* **1996**, 82, 207.
6. Shirakawa, H.; Louis, E.J.; MacDiarmid, A.J.; Chiang, C.K.; Druy, M.N.; Cao, S.C.; Heeger, A.J. *Chem Commun.* **1977**, 578.
7. Dannetun, P.; Lugdlund, M.; Fahlman, M.; Boman, M.; Stafstrom, S.; Salaneck, W.R.; Lazzaroni, R.; Fredriksson, C.; Bredas, J.L.; Grahm, S.; Friend, R.H.; Holmes, A.B.; Zamboni, R.; Taliani, C. *Synth. Met.* **1993**, 55-57, 212.
8. Bantikassegn, W.; Dannetun, P.; Ingnas, O.; Salaneck, W.R. *Synth. Met.* **1993**, 55-57, 36.
9. Bantikassegn, W.; Dannetun, P.; Ingnas, O.; Salaneck, W.R. *Thin Solid Films* **1993**, 224, 232.
10. Salaneck, W.R.; Bredas, J.L. *Adv. Mater.* **1996**, 65, 48, and references therein.
11. Kaniki, J. *Handbook of Conducting Polymers*, Skotheim, T.A. (Ed.), Marcel Dekker: New York; 1986.
12. de Leeuw, D.M.; Lous, E.J. *Synth. Met.* **1994**, 65, 45.
13. Lous, E.J.; Blom, P.W.M.; Molenkamp, L.W.; de Leeuw, D.M. *Phys. Rev. B* **1995**, 51, 17251.
14. Fichou, D.; Horowitz, G.; Nishikitani, Y.; Roncali, J.; Garnier, F. *Synth. Met.* **1989**, 28, C729.
15. Tomozawa, H.; Braun, D.; Phillips, S.D.; Worland, R.; Heeger, A.J. *Synth. Met.* **1989**, 28, C687.
16. Omhori, Y.; Manda, Y.; Takahashi, H.; Kawai, T.; Yashino, K. *Japan. J. Appl. Phys.* **1990**, 29, L837.

17. Gustafsson, G.; Ingnas, O.; Sendberg, M.; Svensson, C. *Synth. Met.* **1991**, 41-43, 449.
18. Assadi, A.; Svensson, C.; Willander, M.; Ingnas, O. *J. Appl. Phys.* **1992**, 72, 2900.
19. Gomes, H.L.; Taylor, D.M.; Underhill, A.E. *Synth. Met.* **1993**, 55-57, 4076.
20. Bantikassegn, W.; Ingnas, O. *Thin Solid Films* **1997**, 293, 138.
21. Bantikassegn, W.; Ingnas, O. *J. Phys. D: Appl. Phys.* **1996**, 29, 2971.
22. Bantikassegn, W.; Ingnas, O. *Synth. Met.* **1997**, 87, 5.
23. Boukamp, B.A. *Equivalent Circuit 4.51*, University of Twente: Enschede, The Netherlands; 1993.
24. Onodera, Y. *Phys. Rev. B* **1984**, 30, 775.
25. Sze, S.M. *Physics of Semiconductor Devices*, Wiley: New York; 1981.
26. Tomozawa, H.; Braun, F.; Phillips, S.; Heeger, A.J.; Kroemer, H. *Synth. Met.* **1987**, 22, 63.
27. Koezuka, H.; Etoh, S. *J. Appl. Phys.* **1983**, 54, 2511.
28. Kumar, A.; Wilisch, W.C.A.; Lewis, N.S. *Crit. Rev. Solid State Mater. Sci.* **1993**, 18, 327.
29. Barus, M.; Donoval, D. *Solid State Electronics* **1993**, 36, 696.
30. Pope, M.; Swenberg, C.E. *Electronic Processes in Organic Crystals*, Oxford University Press: New Yoek; 1982.
31. Cole, K.S.; Cole, R.H. *J. Chem. Phys.* **1941**, 9, 341.
32. Ingnas, O.; Lundstrom, I. *Synth. Met.* **1984/85**, 10, 5.
33. Gustafsson, G.; Sundberg, M.; Ingnas, O.; Svensson, C. *J. Molec. Electron.*, **1990**, 6, 105.
34. Yang, R.; Naoi, K.; Evans, D.F.; Smyrl, W.H.; Hendrickson, W.A. *Langmuir* **1991**, 7, 556.
35. Delabouglise, D. *J. Chim. Phys.* **1995**, 92, 2048.